Editors' Suggestion

Relativistic effects in *ab initio* electron-nucleus scattering

Noemi Rocco,[1] Winfried Leidemann,[2,3] Alessandro Lovato,[3,4] and Giuseppina Orlandini[2,3]
[1]*Department of Physics, University of Surrey, Guildford, GU2 7HX, United Kingdom*
[2]*Dipartimento di Fisica, Universitá di Trento, Via Sommarive 14, I-38123 Trento, Italy*
[3]*INFN-TIFPA Trento Institute of Fundamental Physics and Applications, Via Sommarive, 14, 38123 Trento, Italy*
[4]*Physics Division, Argonne National Laboratory, Argonne, Illinois 60439, USA*

(Received 2 February 2018; published 4 May 2018)

The electromagnetic responses obtained from Green's function Monte Carlo (GFMC) calculations are based on realistic treatments of nuclear interactions and currents. The main limitations of this method comes from its nonrelativistic nature and its computational cost, the latter hampering the direct evaluation of the inclusive cross sections as measured by experiments. We extend the applicability of GFMC in the quasielastic region to intermediate momentum transfers by performing the calculations in a reference frame that minimizes nucleon momenta. Additional relativistic effects in the kinematics are accounted for employing the two-fragment model. In addition, we developed a novel algorithm, based on the concept of first-kind scaling, to compute the inclusive electromagnetic cross section of ^{4}He through an accurate and reliable interpolation of the response functions. A very good agreement is obtained between theoretical and experimental cross sections for a variety of kinematical setups. This offers a promising prospect for the data analysis of neutrino-oscillation experiments that requires an accurate description of nuclear dynamics in which relativistic effects are fully accounted for.

DOI: 10.1103/PhysRevC.97.055501

I. INTRODUCTION

The analysis of neutrino-nucleus interactions in the broad kinematic region relevant for the present [1–4] and future [5,6] generation of neutrino oscillation experiments requires an accurate understanding of nuclear dynamics. The relevance of nuclear models is critical to the reconstruction of the initial neutrino energy, even in experiments where both near and far detectors are present [7]. Recent experimental studies of neutrino-nucleus interactions have provided ample evidence of the inadequacy of the relativistic Fermi gas model, routinely employed in event generators, to describe the observed cross section. The complexity of nuclear dynamics and the variety of reaction mechanisms are such that *ab initio* calculations of nuclear structure and electroweak interactions with nuclei are necessary [8].

Within nuclear *ab initio* approaches the nucleus is treated as an assembly of nucleons interacting with each other via two- and three-body effective potentials [9–15]. The interaction with external electroweak probes is described by one- and two-body effective currents that are consistent with the nuclear interaction. Hence, properties of few-body nuclear systems, such as the nucleon-nucleon (NN) scattering data and the binding energies of light nuclei, ultimately constrain the current operators [16]. This is particularly apparent for the electromagnetic longitudinal current, which is connected to the nuclear potential through the continuity equation.

The Green's function Monte Carlo (GFMC) approach is an *ab initio* method that allows a very accurate description of the structure and low-energy transitions of $A \leqslant 12$ nuclei [17]. More recently, exploiting integral transform techniques, the GFMC method has also been applied to the calculation of the electromagnetic response functions of ^{4}He and ^{12}C, giving a full account of the dynamics of the constituent nucleons in the quasielastic sector. Once two-body currents are accounted for, GFMC predictions are in very good agreement with experimental data [18,19]. However, considering that explicit pion degrees of freedom are not taken into account the strength seems to be somewhat too large beyond the pion threshold.

As a matter of fact, at higher momentum transfer the applicability of GFMC to electroweak scattering and in particular to the analysis of neutrino-nucleus scattering is hampered by its nonrelativistic nature. While leading relativistic corrections are included in the current operators, the quantum mechanical framework is nonrelativistic. The strategy introduced in Ref. [20] to account for relativistic kinematics in nonrelativistic calculations can only be reliably applied to independent particle models of nuclear dynamics.

The inclusion of relativistic corrections in a more sophisticated approach was first discussed in Ref. [21]. The authors argued that performing the nonrelativistic calculation in a specific reference frame can minimize the error introduced by the approximate treatment of relativistic effects. In addition, the frame dependence of nonrelativistic results can be reduced using the so-called two-fragment model to obtain, in a relativistically correct way, the kinematic inputs of the nonrelativistic dynamical calculation . This approach has been successfully employed in the *ab initio* calculation of the electromagnetic longitudinal [21] and transverse [22–25] response functions of ^{3}He at intermediate momentum transfers (up to $|\mathbf{q}| = 700$ MeV).

Following Ref. [21], in this work we gauge the role of relativistic effects in the original GFMC electromagnetic response functions of ^{4}He by studying their frame dependence with and without the two-fragment model.

The GFMC calculations of the response functions and cross sections by neutral-current scattering of neutrinos off ^{12}C have been recently presented in Ref. [26]. In that work, the neutral current differential cross sections have been computed for a single value of the momentum transfer, $|\mathbf{q}| = 570$ MeV, as a function of the energy loss ω. On the other hand, experimental electron- and neutrino-nucleus cross sections are commonly given for fixed values of the incoming beam energy and scattering angle. Their direct evaluation requires one to perform GFMC calculations of the nuclear response functions for several values of $|\mathbf{q}|$, whose computational cost exceeds the current availability. In this work we developed a novel algorithm suitable to compute the double-differential cross sections of electron-^{4}He scattering through an efficient interpolation of the available nuclear responses. The latter exploits the scaling features of the GFMC electromagnetic response functions, which have been recently investigated in Ref. [27]. Using this algorithm and employing the relativistic treatment mentioned above we perform an extensive comparison of our results with the electron scattering data, for initial electron energies ranging from 0.3 to 1.1 GeV.

In Sec. II we briefly review the formalism connecting the electron-nucleus cross section to the longitudinal and transverse response functions and discuss the main elements of their calculation within the GFMC approach. In addition we make a comparison to results obtained with the Lorentz integral transform (LIT) method [28,29]. In Sec. III we review the approach of Ref. [21] to account for relativistic effects and study the frame dependence of the GFMC responses, as well as its reduction with the two-fragment model. Section IV is devoted to the calculation of the electron-^{4}He differential cross sections and to the comparison with experiment. Finally, in Sec. V we draw our conclusions.

II. FORMALISM

In the one-photon-exchange approximation, the inclusive double-differential electron-nucleus cross section can be written in terms of the two response functions $R_L(\mathbf{q},\omega)$ and $R_T(\mathbf{q},\omega)$, describing interactions with longitudinally (L) and transversely (T) polarized virtual photons

$$\frac{d^2\sigma}{dE_{e'}d\Omega_e} = \left(\frac{d\sigma}{d\Omega_e}\right)_{\rm M} [A_L\, R_L(|\mathbf{q}|,\omega) + A_T\, R_T(|\mathbf{q}|,\omega)], \quad (1)$$

where

$$A_L = \left(\frac{q^2}{\mathbf{q}^2}\right)^2, \quad A_T = -\frac{1}{2}\frac{q^2}{\mathbf{q}^2} + \tan^2\frac{\theta_e}{2}, \quad (2)$$

and

$$\left(\frac{d\sigma}{d\Omega_e}\right)_{\rm M} = \left[\frac{\alpha\cos(\theta_e/2)}{2E_{e'}\sin^2(\theta_e/2)}\right]^2 \quad (3)$$

is the Mott cross section. In the above equation $\alpha \simeq 1/137$ is the fine structure constant, E'_e and θ_e are the final lepton energy and scattering angle, respectively, $\mathbf{q}$ and ω are energy and momentum transferred by the electron to the target nucleus, and $q^2 = \omega^2 - \mathbf{q}^2$.

The longitudinal and transverse response functions are expressed in terms of the nuclear current matrix elements

$$R_\alpha(|\mathbf{q}|,\omega) = \sum_f \langle 0|j^\dagger_\alpha(\mathbf{q},\omega)|f\rangle\langle f|j_\alpha(\mathbf{q},\omega)|0\rangle \times \delta(\omega - E_f + E_0), \quad (4)$$

where $|0\rangle$ and $|f\rangle$ represent the nuclear initial ground state and final bound or scattering state of energies E_0 and E_f, and $j_\alpha(\mathbf{q},\omega)$ ($\alpha = L,T$) denotes the longitudinal and transverse components of the electromagnetic current. For moderate momentum transfer, corresponding to $|\mathbf{q}| \lesssim 500$ MeV, nonrelativistic nuclear many-body theory can be applied to consistently describe the initial and the final scattering states in the quasielastic peak region. To this aim, a nonrelativistic reduction of the electromagnetic currents, which includes one- and two-body terms consistent with the nuclear Hamiltonian, is performed. The explicit expressions for the electromagnetic currents employed in this work can be found in Ref. [30].

A. GFMC approach to response functions

Following the strategy adopted in Refs. [18,19,31], instead of attempting a direct calculation of each individual transition amplitude $|0\rangle \to |f\rangle$, we exploit integral transform techniques to reduce the problem to a ground-state one. In particular, we evaluate the inelastic Euclidean responses, defined through the following Laplace transform of the electromagnetic response functions:

$$E_\alpha(|\mathbf{q}|,\tau) = \int_{\omega^+_{\rm el}}^\infty d\omega R_\alpha(|\mathbf{q}|,\omega)e^{-\omega\tau}, \quad (5)$$

where $\omega_{\rm el}$ is the energy of the recoiling ground state. Besides the energy-conserving δ function, the response functions depend upon ω through the electromagnetic form factors of the nucleon and N-to-Δ transition in the currents. We artificially remove these dependences by evaluating the form factors at the quasielastic peak $q^2_{\rm qe} = \omega^2_{\rm qe} - \mathbf{q}^2$. Exploiting the completeness of the final states of Eq. (4), the inelastic Euclidean responses can be written as the following ground-state expectation value:

$$E_\alpha(|\mathbf{q}|,\tau) = \langle\Psi_0|j^\dagger_\alpha(\mathbf{q},\omega_{\rm qe})e^{-(H-E_0)\tau}\, j_\alpha(\mathbf{q},\omega_{\rm qe})|\Psi_0\rangle - |F_\alpha(q)|^2\, e^{-\tau\omega_{\rm el}}, \quad (6)$$

where $F_\alpha(q)$ is the longitudinal elastic form factor and H the nuclear Hamiltonian. For its potential part we use the Argonne v_{18} (AV18) [32] NN potential and Illinois-7 (IL7) [33] three-nucleon force (3NF). The Simon [34], Galster [35], and Höhler [36] parametrizations are used for the proton electric, neutron electric, and proton and neutron magnetic form factors, respectively.

In order to reduce the computational cost and to evaluate the terms in the currents that depend upon the momentum of the nucleon, we use our best variational trial wave function $|\Psi_T\rangle$ for $|\Psi_0\rangle$. Hence, the response functions are those obtained from $|\Psi_T\rangle$ rather than those from the evolved GFMC wave function. However, the sum rule results of Ref. [37] indicate that this is indeed a good approximation.

The calculation of this ground-state expectation value is carried out in two steps. At first the unconstrained imaginary-time

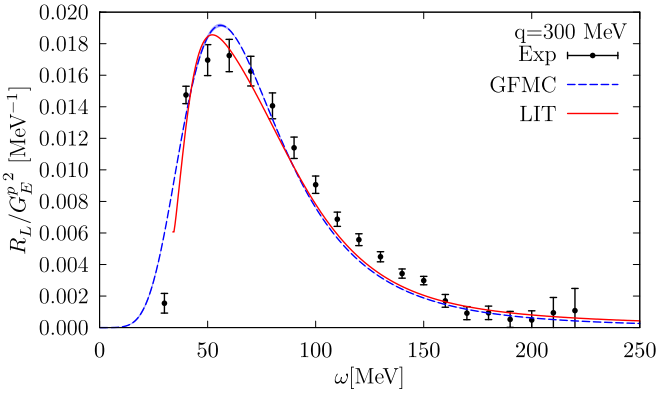

FIG. 1. Longitudinal electromagnetic response functions of ^{4}He at $|\mathbf{q}| = 300$ MeV obtained inverting the Laplace and Lorentz integral transforms compared to the experimental data of Ref. [31].

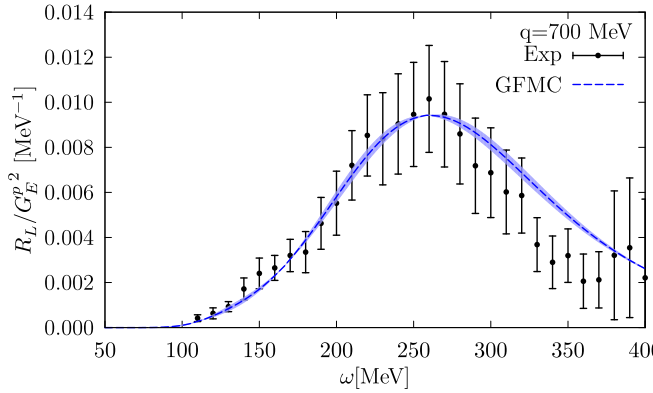

FIG. 2. GFMC longitudinal electromagnetic response function of ^{4}He at $|\mathbf{q}| = 700$ MeV. Experimental data are from Ref. [31].

propagation of $|\Psi_T\rangle$ is performed and stored. Then, the states obtained from $j_\alpha(\mathbf{q},\omega_{\rm qe})|\Psi_T\rangle$ are propagated in imaginary time and the scalar product of $e^{-(H-E_0)\tau}\, j_\alpha(\mathbf{q},\omega_{\rm qe})|\Psi_T\rangle$ with $\langle\Psi_T|j_\alpha^\dagger(\mathbf{q},\omega_{\rm qe})$ is performed on a grid of τ_i values (for more details see Refs. [15,18,31]). The inversion of the Laplace transform, needed to retrieve the response functions, is performed exploiting maximum entropy techniques, as described in Ref. [19].

B. Comparison with Lorentz integral transform results

To test the reliability of the GFMC calculation and in particular of the inversion procedure, in Fig. 1 we compare the longitudinal response function of ^{4}He divided by the proton electric form factor squared with that obtained in Refs. [38,39] employing the LIT method. The latter was computed representing $|0\rangle$ and the LIT states $\tilde{\Psi}$ (see Ref. [28]) in terms of hyperspherical harmonics. The Hamiltonian used in that case was the NN AV18 potential and the Urbana IX (UIX) 3NF. The agreement with experimental data, taken from Ref. [31] is remarkably good. The two theoretical curves are also in very good agreement. The small discrepancies can be ascribed to (i) the different 3NF models employed, (ii) the very narrow isoscalar monopole resonance contribution (see [40]) that was subtracted from the LIT, (iii) the spin-orbit correction in the longitudinal current operator that is only included in the GFMC results, and (iv) the use of a variational Monte Carlo ground state. Finally, it has to be noted that resolving the low-energy transfer region of the response requires imaginary-time evolution to large values of τ, which is hampered by the fermion sign problem.

At $|\mathbf{q}| = 500$ MeV the difference between LIT and GFMC results becomes somewhat more pronounced. It mainly consists of a slightly shifted quasielastic peak position. We checked that the origin of the difference is not due to an inversion problem. In fact, in addition to the standard LIT inversion method [41], we used the maximum entropy technique to invert the LIT. We did not find significant differences in the resulting R_L. It remains the object of further future investigations as to whether the differences can be explained by items (i)–(iv) mentioned above.

III. INCLUSION OF RELATIVISTIC EFFECTS

In Fig. 2 we compare the GFMC longitudinal response function of ^{4}He divided by the proton electric form factor of Ref. [36] squared with the corresponding experimental data for $|\mathbf{q}| = 700$ MeV. We notice a slight shift of the position of the quasielastic peak to higher ω and an overestimation of its width. Here one has to take into account that although relativistic corrections up to order q^2/m^2, where m is the mass of the nucleon, are included in the current operator for R_L, the quantum mechanical approach—and hence the kinematics—is nonrelativistic. Strategies allowing to tackle relativistic corrections do exist in mean-field approaches [20]; however, an inclusion of relativistic effects in a fully interacting nuclear many-body system is highly nontrivial. To cope with this problem, in the following, we will use the approach mentioned in the Introduction.

In Refs. [21–25], it was proposed that one should perform the nonrelativistic calculation in a specific reference frame, where relativistic effects are as small as possible. For example, in electron-nucleon scattering one prefers the Breit system, where the initial nucleon is moving with $-\mathbf{q}/2$. A generalization to the quasielastic region in electron-nucleus scattering, which is dominated by a one-nucleon knockout, leads to the so-called active nucleon Breit (ANB) frame, where the target nucleus moves with a momentum of $-A\,\mathbf{q}/2$. In this frame, any of the A nucleons composing the nucleus in the initial state has a momentum of about $-\mathbf{q}/2$, while the knocked-out nucleon carries a momentum $\simeq \mathbf{q}/2$ after the reaction. In any other reference frame the involved momenta are higher. For example, in the laboratory (LAB) system the knocked-out nucleon has a momentum of about $\mathbf{q}$, hence relativistic effects can be minimized using the ANB system.

Since experiments are carried out in the LAB system, it is necessary to transform the results from the ANB (or any other frame where one performs the nonrelativistic calculation) to the LAB frame. For reference frames moving with respect to the LAB frame along the $\mathbf{q}$ direction, as is the case for the ANB frame, the responses transform as follows:

$$R_L(|\mathbf{q}|,\omega) = \frac{\mathbf{q}^2}{(\mathbf{q}^{\rm fr})^2}\,\frac{\sqrt{M_T^2 + \left(\mathbf{P}_i^{\rm fr}\right)^2}}{M_T}\,R_L(|\mathbf{q}^{\rm fr}|,\omega^{\rm fr}), \qquad (7)$$

$$R_T(|\mathbf{q}|,\omega) = \frac{\sqrt{M_T^2 + \left(\mathbf{P}_i^{\rm fr}\right)^2}}{M_T} R_T(|\mathbf{q}^{\rm fr}|,\omega^{\rm fr}). \quad (8)$$

In the above equations M_T is the mass of the target nucleus while $|\mathbf{q}^{\rm fr}|$ and $\omega^{\rm fr}$ are the momentum transfer and the energy transfer pertaining to the reference frame under consideration, namely,

$$\mathbf{q}^{\rm fr} = \mathbf{P}_f^{\rm fr} - \mathbf{P}_i^{\rm fr}, \quad \omega^{\rm fr} = E_f^{\rm fr} - E_i^{\rm fr}, \quad (9)$$

where the total nonrelativistic energies $E_{i/f}^{\rm fr}$ are given by

$$E_i^{\rm fr} = \frac{\left(\mathbf{P}_i^{\rm fr}\right)^2}{2M_T} + \epsilon_0, \quad E_f^{\rm fr} = \frac{\left(\mathbf{P}_f^{\rm fr}\right)^2}{2M_T} + \epsilon_f, \quad (10)$$

with $\mathbf{P}_{i/f}^{\rm fr}$ indicating the center-of-mass momenta in the specified reference frame. Since in a nonrelativistic calculation the intrinsic system does not depend on the center-of-mass momentum, the intrinsic energies ϵ_f and ϵ_0 are assumed to be frame independent.

At first, we perform GFMC calculations for a number of momentum transfers of the intrinsic response functions, defined as

$$R_\alpha^{\rm int}(|\mathbf{q}^{\rm fr}|,\omega^{\rm int}) = \sum_f \langle 0|j_\alpha^\dagger(\mathbf{q}^{\rm fr},\omega^{\rm int})|f\rangle \times \langle f|j_\alpha(\mathbf{q}^{\rm fr},\omega^{\rm int})|0\rangle \delta(\omega^{\rm int} - \epsilon_f + \epsilon_0). \quad (11)$$

The direct calculation of the response functions in the LAB frame is simply achieved by taking $\mathbf{q}^{\rm fr} = \mathbf{q}$ and $\omega^{\rm int} = \omega - \mathbf{q}^2/(2M_T)$. On the other hand, to determine the responses in the LAB frame from Eqs. (7) and (8), $|\mathbf{q}|^{\rm fr}$ and $\omega^{\rm fr}$ are computed with the appropriate Lorentz transformation from $|\mathbf{q}|$ and ω. If $|\mathbf{q}^{\rm fr}|$ does not correspond to any of the tabulated momentum transfers, the response $R_{L/T}(|\mathbf{q}^{\rm fr}|,\omega^{\rm fr})$ is obtained interpolating the intrinsic response function using the procedure described in Sec. IV for $\omega^{\rm int} = \omega^{\rm fr} - (\mathbf{P}_f^{\rm fr})^2/(2M_T) + (\mathbf{P}_i^{\rm fr})^2/(2M_T)$.

Two-fragment model

Relativistic effects in the kinematics can be included employing the two-fragment model of Ref. [21]. This relies on the assumption that the quasielastic reaction is dominated by the break-up of the nucleus into two fragments, namely a knocked-out nucleon and a remaining $(A-1)$ system in its ground state. This assumption enables one to connect $\omega^{\rm fr}$ to the intrinsic excitation energy ϵ_f used in the nonrelativistic calculation in a relativistically correct way. It has to be noted that the two-fragment model is adopted only for determining the kinematic input of a calculation where the full nuclear dynamics of the system is taken into account.

At this point, we recall that within nonrelativistic theory it is not possible to work simultaneously with the correct relativistic energy and momentum of a two-fragment system. As pointed out in [21], a clue comes from the two-nucleon case. In fact, NN potential models are constructed describing the two-nucleon relative scattering momentum p_{12} in a relativistically correct way, whereas the Schrödinger equation is solved for the "fake" nonrelativistic kinetic energy $E_{12} = p_{12}^2/2\mu_{12}$, where μ_{12} is the reduced mass of the two nucleons. (The same approach is also used in deuteron electrodisintegration, see, e.g., [42]).

Proceeding analogously to the NN potential case, the two-fragment kinematical model can be summarized by the following points:

(a) The choice of the frame defines $\mathbf{P}_i^{\rm fr}$, and accordingly also the initial relativistic hadron energy

$$E_i^{\rm fr} = \sqrt{M_T^2 + \left(\mathbf{P}_i^{\rm fr}\right)^2}. \quad (12)$$

(b) The momenta of the knocked-out nucleon and the spectator system are set equal to $\mathbf{p}_N^{\rm fr}$ and $\mathbf{p}_X^{\rm fr}$, respectively. The corresponding relative and center-of-mass momenta are obtained as

$$\mathbf{p}_{\rm f}^{\rm fr} = \mu\left(\frac{\mathbf{p}_N^{\rm fr}}{m} - \frac{\mathbf{p}_X^{\rm fr}}{M_X}\right), \quad (13)$$

$$\mathbf{P}_f^{\rm fr} = \mathbf{p}_N^{\rm fr} + \mathbf{p}_X^{\rm fr}, \quad (14)$$

where M_X and μ are the mass of the spectator system and the reduced mass, respectively.

(c) For reference frames moving with respect to the LAB frame along the $\mathbf{q}^{\rm fr}$ direction, $\mathbf{P}_f^{\rm fr}$ is directed along $\mathbf{q}^{\rm fr}$. In addition, for a quasielastic reaction one can safely assume that also $\mathbf{p}^{\rm fr}$ is directed along $\mathbf{q}^{\rm fr}$. Therefore $\mathbf{p}_f^{\rm fr}$ and $\mathbf{P}_f^{\rm fr}$ have the same direction. Under this assumption, $p_f^{\rm fr}$ can be obtained from the relativistically correct final state energy of the hadron system

$$E_f^{fr} = \sqrt{m^2 + \left(\mathbf{p}_f^{\rm fr} + (\mu/M_{A-1})\mathbf{P}_f^{\rm fr}\right)^2} + \sqrt{M_{A-1}^2 + \left(\mathbf{p}_f^{\rm fr} - (\mu/m)\mathbf{P}_f^{\rm fr}\right)^2}. \quad (15)$$

(d) For each value of $\omega^{\rm fr}$ and $q^{\rm fr}$, one obtains $P_f^{\rm fr}$ and $E_f^{\rm fr}$ from Eq. (9). The relativistic relative momentum of the two fragments is determined by plugging Eq. (15) into Eq. (9). This then leads to the determination of the intrinsic energy

$$\epsilon_f = \frac{\left(p_f^{\rm fr}\right)^2}{2\mu} + \epsilon_0^{A-1}, \quad (16)$$

where $(p_f^{\rm fr})^2/2\mu$ is the relativistically "fake" kinetic energy and ϵ_0^{A-1} the ground-state energy of the spectator system. Finally, the response function of the two-body fragment model can be computed interpolating the intrinsic response of Eq. (11) at

$$\omega^{\rm int} = \frac{\left(p_f^{\rm fr}\right)^2}{2\mu} - \epsilon_0 + \epsilon_0^{A-1}. \quad (17)$$

As further discussed in [21] one also has to rescale the response functions [see Eqs. (9)–(11) therein]. At this point one transforms the results to the LAB system as described above for the case without the two-fragment model.

Using the LIT method, the two-fragment model has been applied to the calculation of the ^{3}He longitudinal [21] and transverse response functions [24,25]. Meson exchange and Δ isobar currents as well as relativistic corrections of order $\mathbf{q}^2/m^2$ for the one-body charge and current operators were included. There it was shown that the large frame dependence of the results is almost eliminated by the use of the two-fragment

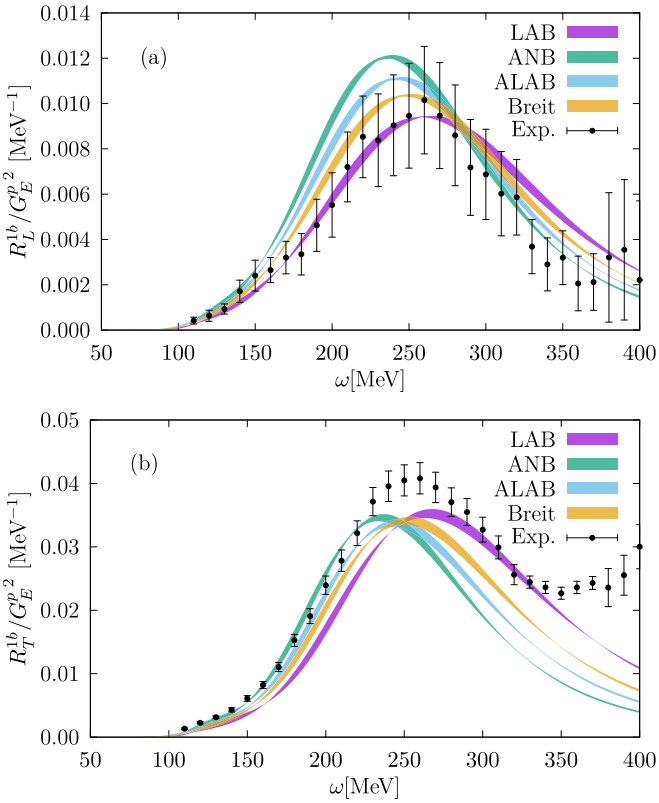

FIG. 3. Frame dependence of the GFMC longitudinal (a) and transverse (b) electromagnetic response functions of ^{4}He at $|\mathbf{q}| =$ 700 MeV.

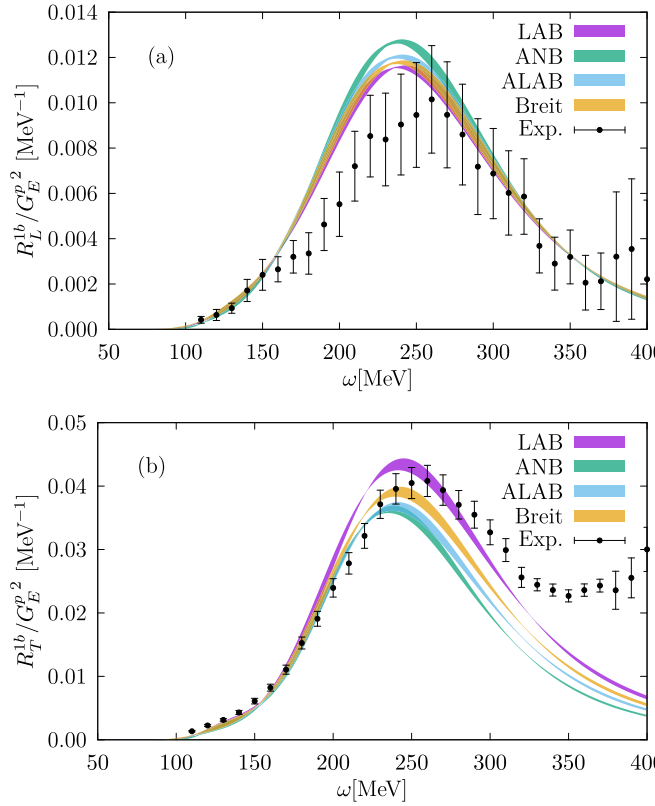

FIG. 4. Same as Fig. 3, but considering two-body relativistic kinematics for the final state energy.

relativistic kinematics, even considering momentum transfers up to $|\mathbf{q}| = 700$ MeV. In particular a considerable shift of the quasielastic peak was found for all reference frames but the ANB one. An excellent description of experimental ^{3}He(e,e') data is achieved when making the calculation in the ANB frame supplementing it with the two-fragment model.

In this work, we have calculated the GFMC electromagnetic responses of the four-body system in the same reference frames as in [21,24,25]. For $|\mathbf{q}| = 700$ MeV we obtain the results shown in Fig. 3(a) for the longitudinal and Fig. 3(b) for the transverse channels. As in the three-body case, a rather strong frame dependence can be noticed, indicating that relativistic effects play a non-negligible role at this value of the momentum transfer. The corresponding results obtained employing the two-fragment model are displayed in Fig. 4. The position of the quasielastic peak of the electromagnetic responses no longer depends upon the reference frame and coincides with that of the ANB frame of Fig. 3. While in the longitudinal channel the different curves are almost coincident, the transverse responses still suffer a residual frame dependence, leading to different heights of the quasielastic peak. This has to be ascribed to the fact that, at variance with Ref. [24], the subleading relativistic corrections in the transverse current operator are neglected in the GFMC calculations. Our results are consistent with the findings of Ref. [43], where the role of relativistic effects in the kinematics and in the current operator is separately analyzed. In the LAB frame using relativistic currents brings about a reduction of the strength of the transverse response compared to the nonrelativistic ones. This effect is expected to be smaller in the ANB frame, where the ω-dependent correction in the current considered in Ref. [24] vanishes at the quasielastic peak.

There is a fairly good agreement between theory and experiment for the position of the quasielastic peak, in both the longitudinal and the transverse channels. As for the peak heights, in the longitudinal case our calculations slightly overestimate the experimental data, consistently with Ref. [21] for the ^{3}He case. In the transverse channel, for the afore-mentioned missing relativistic corrections in the current operator, only the ANB predictions can be meaningfully compared with experiments. Here, excess strength from meson-exchange two-body currents is needed to bring GFMC results in agreement with experiments even in the quasielastic peak region.

IV. FROM RESPONSE FUNCTIONS TO CROSS SECTIONS

The calculation of the inclusive electron-nucleus scattering cross section of Eq. (1) requires the knowledge of R_L and R_T for several values of ω and $|\mathbf{q}|$. Hence, due to the sizable computational effort required to accurately invert the Euclidean response for a given value of $|\mathbf{q}|$, the direct evaluation made with Eq. (1) is not feasible within GFMC. To circumvent these difficulties, we developed a novel interpolation algorithm based on the scaling of the nuclear responses. The latter has been introduced and widely analyzed in the framework of the

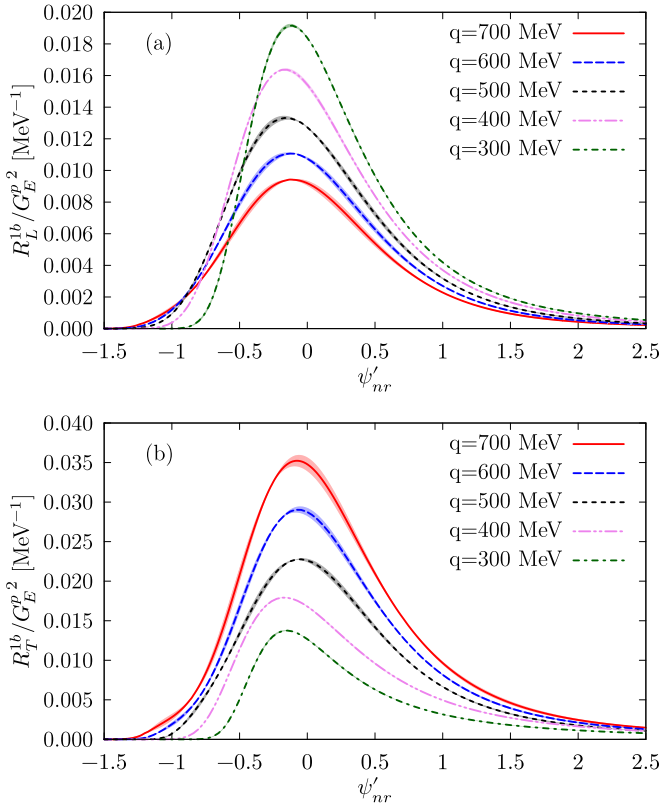

FIG. 5. One-body longitudinal (a) and transverse (b) electromagnetic response functions of ^{4}He for $|\mathbf{q}_i| = 300$, 400, 500, 600, and 700 MeV as a function $\psi'_{\rm nr}$ given in Eq. (18).

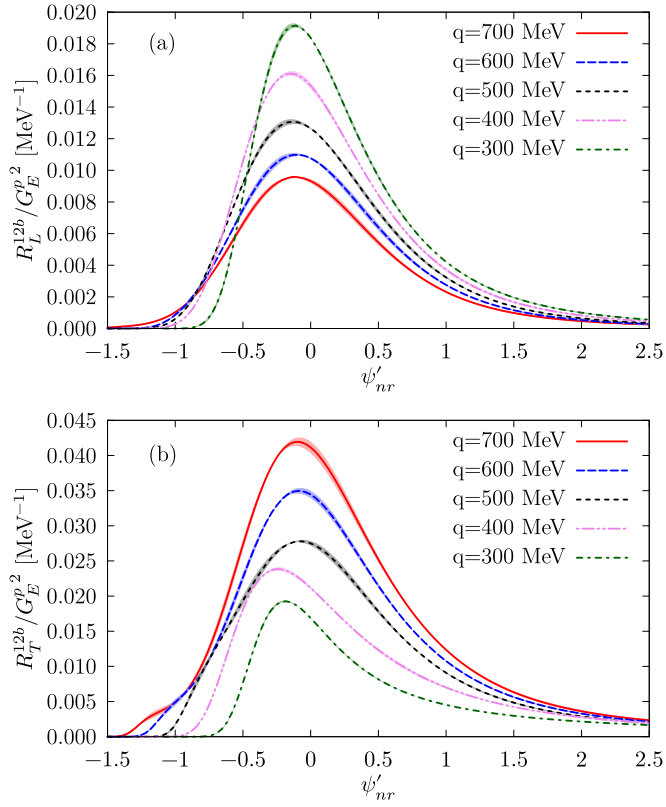

FIG. 6. Same as in Fig. 5, but including one- and two-body terms in the electromagnetic current.

global relativistic Fermi gas (GRFG) model [44,45]. Scaling of the first kind occurs when the response functions divided by an appropriate factor, which accounts for single-nucleon physics, no longer depend on $\mathbf{q}$ and ω, but only upon a specific function of them, which defines the scaling variable ψ. Recently, the authors of Ref. [27] carried out an analysis of the scaling features of the GFMC electromagnetic response functions of ^{4}He and ^{12}C, retaining only one-body current contributions. Their results show that scaling is fulfilled, provided that the nonrelativistic scaling variable $\psi^{\rm nr}$ is used. The latter is obtained from the nonrelativistic reduction of the energy-conserving δ function of Eq. (4), assuming that the scattering process takes place on a single nucleon and using the free energy spectrum for the initial and final states. In this work, we introduce a constant shift in the energy transfer in the definition of the scaling variable

$$\psi'_{\rm nr} = p_F\left(\frac{\omega - E_s}{|\mathbf{q}|} - \frac{|\mathbf{q}|}{2m}\right). \tag{18}$$

In the above equation, p_F is the Fermi momentum, and E_s is empirically chosen to account for binding effects in both the initial and final states. In the present analysis of the ^{4}He nucleus, we use $p_F = 180$ MeV and $E_s = 15$ MeV. However, the results are quite insensitive to small variations of these parameters.

Figure 5(a) shows the longitudinal and Fig. 5(b) the transverse response functions of ^{4}He divided by the proton electric form factor squared for $|\mathbf{q}_i| = 300$, 400, 500, 600, and 700 MeV as a function $\psi'_{\rm nr}$. In both channels the curves corresponding to different values of the momentum transfer peak around $\psi'_{\rm nr} = 0$ and the height of the quasielastic peaks is a monotonic function of $|\mathbf{q}|$. In the longitudinal case, shown in Fig. 5(a), the highest and the lowest peak correspond to $|\mathbf{q}| = 300$ and 700 MeV, respectively. On the other hand, in the transverse channel, displayed in Fig. 5(b), the response functions are smaller as $|\mathbf{q}|$ decreases. In Fig. 6 both one- and two-body terms in the electromagnetic current have been included. Meson-exchange current contributions only appreciably affect the transverse channel, leading to a sizable enhancement of the response functions. Nevertheless, the behavior of the curves in both panels is analogous to that of Fig. 5.

To evaluate Eq. (1) we fix E_e and θ_e, the initial electron beam energy and scattering angle, respectively, and use $E_{e'} = E_e - \omega$ for the energy of the outgoing electron. The four-momentum transfer is then written as

$$Q^2 = -q^2 = 4E_e(E_e - \omega)\sin^2\frac{\theta_e}{2}. \tag{19}$$

For a given value of ω, the response functions have to be evaluated at $|\mathbf{q}| = \sqrt{\omega^2 + Q^2}$. To this aim, we first compute $\psi'_{\rm nr}$ as in Eq. (18). Then, the set of $R_{L,T}(\psi'_{\rm nr}, q_i)$ is interpolated at $|\mathbf{q}|$. By looking at Figs. 5 and 6, it becomes evident why it is more convenient to interpolate the different response functions when the latter are given as a function of $\psi'_{\rm nr}$ and $|\mathbf{q}|$ rather than ω and $|\mathbf{q}|$. For a given value of $\psi'_{\rm nr}$ the curves corresponding

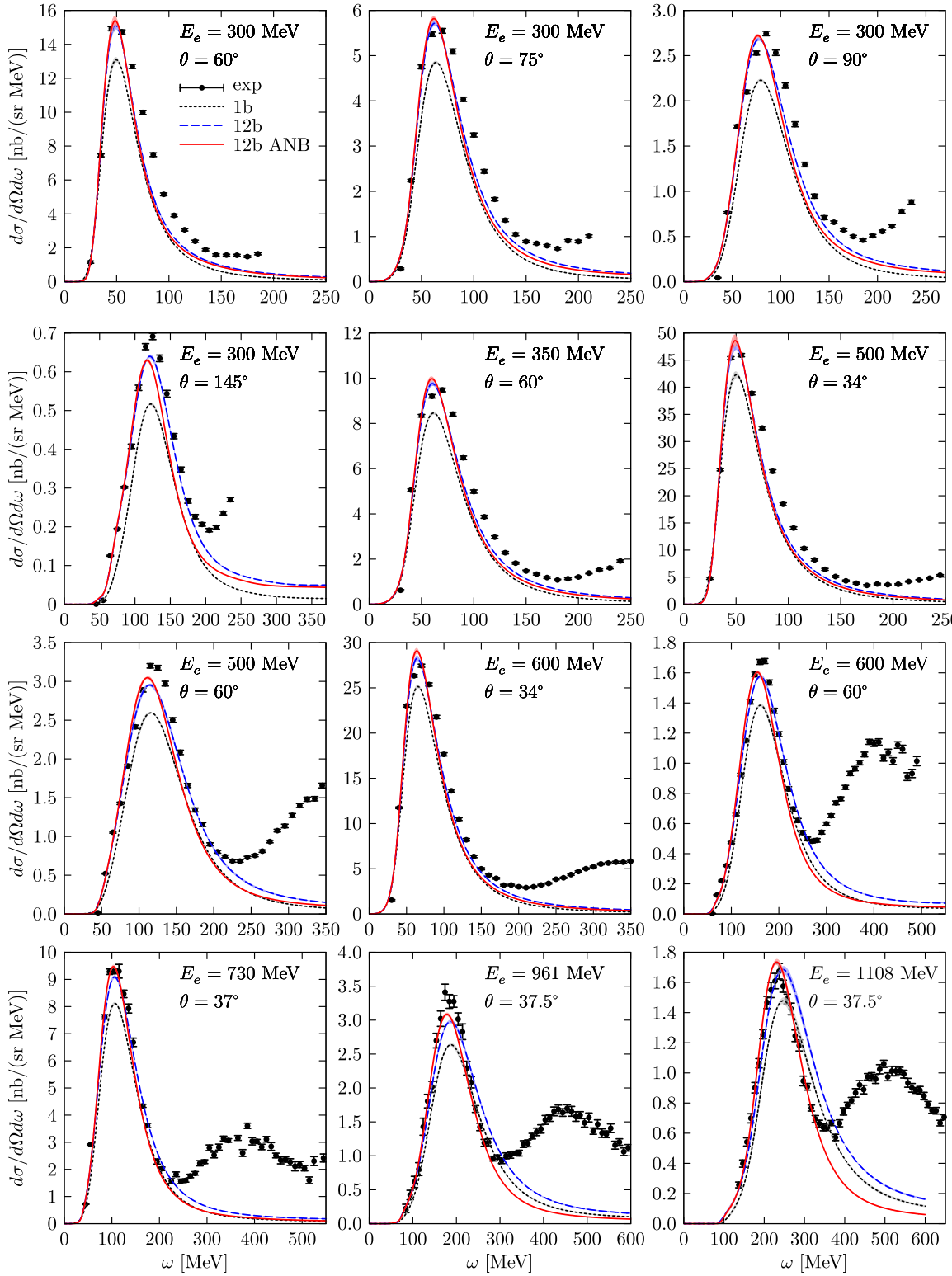

FIG. 7. Double-differential electron-^{4}He cross sections for different values of incident electron energy and scattering angle. The dotted-black and dashed-blue lines correspond to GFMC calculations where only one-body and one- plus two-body contributions in the electromagnetic currents are accounted for. The red-solid line indicates one- plus two-body current results obtained in the ANB frame, employing the two-body fragment model to account for relativistic kinematics. The experimental data are taken from Ref. [46].

to the different $|\mathbf{q}_i|$ are indeed almost perfectly aligned and monotonic functions of $|\mathbf{q}|$, largely improving the accuracy of the interpolation procedure.

In Fig. 7 we compare with experimental data the electron-^{4}He inclusive double-differential cross sections obtained from the GFMC responses for various kinematic setups, corresponding to different values of E_e and θ_e. The dotted-black and dashed-blue curves correspond to retaining only one-body terms or both one- and two-body terms in the current operators. The red-solid curves—which account for the contribution of one- plus two-body current operators—have been obtained computing the cross section in the ANB frame employing the two-fragment model to account for relativistic kinematics, and boosting back to the LAB frame.

Our findings are consistent with those of Ref. [18], as we observe that the two-body currents generate a large excess of strength over the whole ω spectrum, largely improving the agreement with experimental data. The difference between the red and blue curves is clearly visible for $E_e = 961$, 1080 MeV and $\theta_e = 37.5^\circ$, where $Q^2 \gtrsim 3$ GeV^2 at the quasielastic peak. In these two kinematic setups, the inclusion of relativistic corrections lead to a shift in the position of the quasielastic peak and a reduction of its width. The latter effect is needed to not overestimate the experimental data once the resonance production mechanism is accounted for.

V. CONCLUSIONS

The electromagnetic longitudinal responses of ^{4}He obtained with the GFMC have been successfully benchmarked with some LIT results from the literature [38,39]. For $|\mathbf{q}| =$ 300 MeV we have found a very good agreement between the two theoretical *ab initio* approaches. We have checked that the small discrepancies, which become more pronounced at $|\mathbf{q}| = 500$ MeV, are not due to problems pertaining to the inversion procedure. They are likely to be ascribed to various smaller differences in the calculations listed in Sec. II B.

We have gauged the relativistic effects in the GFMC electromagnetic response functions at relatively high value of the momentum transfer, $|\mathbf{q}| = 700$ MeV. To this aim, we have computed the response functions in different reference frames, boosting the results back to the LAB frame. We observe sizable differences in the position and strength of the quasielastic peak. The two-fragment model of Ref. [21], suitable for realistic models of nuclear dynamics, has been employed to account for relativistic kinematics. This method has proven to provide fully satisfactory results in the longitudinal channel. As for the transverse channel, residual frame dependence in the strength of the quasielastic peak is likely to be due to the missing higher-order relativistic corrections in the transition operator. This is consistent with the findings of Refs. [24,43] and their inclusion will be the subject of future work.

A novel algorithm to reliably and efficiently interpolate the GFMC response functions for arbitrary values of $|\mathbf{q}|$ and ω has been devised. This algorithm relies on the first-kind scaling features of the GFMC responses, which have been analyzed in Ref. [27]. It has to be noted that scaling violations do not prevent its application. On the other hand, if scaling were exactly fulfilled, the algorithm would only require the GFMC calculation of the response functions for a single value of $|\mathbf{q}|$.

We have employed the interpolation algorithm to perform the first *ab initio* calculation of the double-differential cross section of the inclusive electron-^{4}He scattering. The extensive comparison with experimental data demonstrates that two-body currents generate an excess of strength that is necessary to correct the cross section, even in the quasielastic peak region. Relativistic corrections, only appreciable for larger values of the lepton energy and scattering angles, lead to a shift in the position of the quasielastic peak and a reduction of its width. Our findings indicate that relativistic effects are primarily kinematical in nature and can easily be accounted for in the GFMC or any nuclear *ab initio* approach, provided that the many-body calculations are carried out in a proper reference frame. Therefore the fact that neutrino fluxes in current and planned experiments cover a broad energy range extending to several GeVs does not invalidate per se the results obtained within the nonrelativistic approach.

ACKNOWLEDGMENTS

Many illuminating discussions with S. Bacca, J. Carlson, J. Nieves, and R. Schiavilla are gratefully acknowledged. This research has been supported by the U.S. Department of Energy, Office of Science, Office of Nuclear Physics, under Contract No. DE-AC02-06CH11357, and by the Centro Nazionale delle Ricerche (CNR) and the Royal Society under the CNR-Royal Society International Fellowship scheme NF161046. Under an award of computer time provided by the INCITE program, this research used resources of the Argonne Leadership Computing Facility at Argonne National Laboratory, which is supported by the Office of Science of the U.S. Department of Energy under Contract No. DE-AC02-06CH11357.

[1] The MINERνA Experiment, http://minerva.fnal.gov.
[2] The MicroBooNE Experiment, http://www-microboone.fnal.gov.
[3] The NOvA Experiment, http://www-nova.fnal.gov.
[4] The T2K Experiment, http://t2k-experiment.org.
[5] The Deep Underground Neutrino Experiment, http://www.dunescience.org.
[6] Hyper-Kamiokande, http://www.hyperk.org.
[7] T. Katori and M. Martini, J. Phys. G **45**, 013001 (2018).
[8] O. Benhar, P. Huber, C. Mariani, and D. Meloni, Phys. Rep. **700**, 1 (2017).
[9] W. Leidemann and G. Orlandini, Prog. Part. Nucl. Phys. **68**, 158 (2013).
[10] B. R. Barrett, P. Navratil, and J. P. Vary, Prog. Part. Nucl. Phys. **69**, 131 (2013).
[11] G. Hagen, T. Papenbrock, M. Hjorth-Jensen, and D. J. Dean, Rep. Prog. Phys. **77**, 096302 (2014).
[12] H. Hergert, S. K. Bogner, T. D. Morris, A. Schwenk, and K. Tsukiyama, Phys. Rep. **621**, 165 (2016).
[13] A. Carbone, A. Cipollone, C. Barbieri, A. Rios, and A. Polls, Phys. Rev. C **88**, 054326 (2013).

[14] E. Epelbaum, H. Krebs, D. Lee, and Ulf-G. Meißner, Phys. Rev. Lett. **106**, 192501 (2011).
[15] J. Carlson, S. Gandolfi, F. Pederiva, S. C. Pieper, R. Schiavilla, K. E. Schmidt, and R. B. Wiringa, Rev. Mod. Phys. **87**, 1067 (2015).
[16] H.-W. Hammer, A. Nogga, and A. Schwenk, Rev. Mod. Phys. **85**, 197 (2013)
[17] J. Carlson, Phys. Rev. C **36**, 2026 (1987).
[18] A. Lovato, S. Gandolfi, J. Carlson, S. C. Pieper, and R. Schiavilla, Phys. Rev. C **91**, 062501 (2015).
[19] A. Lovato, S. Gandolfi, J. Carlson, S. C. Pieper, and R. Schiavilla, Phys. Rev. Lett. **117**, 082501 (2016).
[20] J. E. Amaro, M. B. Barbaro, J. A. Caballero, T. W. Donnelly, and C. Maieron, Phys. Rev. C **71**, 065501 (2005).
[21] V. D. Efros, W. Leidemann, G. Orlandini, and E. L. Tomusiak, Phys. Rev. C **72**, 011002 (2005).
[22] V. D. Efros, W. Leidemann, G. Orlandini, and E. L. Tomusiak, Phys. Rev. C **81**, 034001 (2010).
[23] L. P. Yuan, V. D. Efros, W. Leidemann, and E. L. Tomusiak, Phys. Rev. C **82**, 054003 (2010).
[24] V. D. Efros, W. Leidemann, G. Orlandini, and E. L. Tomusiak, Phys. Rev. C **83**, 057001 (2011).
[25] L. Yuan, W. Leidemann, V. D. Efros, G. Orlandini, and E. L. Tomusiak, Phys. Lett. B **706**, 90 (2011).
[26] A. Lovato, S. Gandolfi, J. Carlson, E. Lusk, S. C. Pieper, and R. Schiavilla, Phys. Rev. C **97**, 022502 (2018).
[27] N. Rocco, L. Alvarez-Ruso, A. Lovato, and J. Nieves, Phys. Rev. C **96**, 015504 (2017).
[28] V. D. Efros, W. Leidemann, and G. Orlandini, Phys. Lett. B **338**, 130 (1994).
[29] V. D. Efros, W. Leidemann, G. Orlandini, and N. Barnea, J. Phys. G **34**, R459(R) (2007).
[30] G. Shen, L. E. Marcucci, J. Carlson, S. Gandolfi, and R. Schiavilla, Phys. Rev. C **86**, 035503 (2012).
[31] J. Carlson, J. Jourdan, R. Schiavilla, and I. Sick, Phys. Rev. C **65**, 024002 (2002).
[32] R. B. Wiringa, V. G. J. Stoks, and R. Schiavilla, Phys. Rev. C **51**, 38 (1995).
[33] S. C. Pieper and R. B. Wiringa, Ann. Rev. Nucl. Part. Sci. **51**, 53 (2001).
[34] G. G. Simon, C. Schmitt, F. Borkowski, and V. H. Walther, Nucl. Phys. A **333**, 381 (1980).
[35] S. Galster, H. Klein, J. Moritz, K. H. Schmidt, D. Wegener, and J. Bleckwenn, Nucl. Phys. B **32**, 221 (1971).
[36] G. Hohler, E. Pietarinen, I. Sabba Stefanescu, F. Borkowski, G. G. Simon, V. H. Walther, and R. D. Wendling, Nucl. Phys. B **114**, 505 (1976).
[37] A. Lovato, S. Gandolfi, R. Butler, J. Carlson, E. Lusk, S. C. Pieper, and R. Schiavilla, Phys. Rev. Lett. **111**, 092501 (2013).
[38] S. Bacca, N. Barnea, W. Leidemann, and G. Orlandini, Phys. Rev. Lett. **102**, 162501 (2009).
[39] S. Bacca, N. Barnea, W. Leidemann, and G. Orlandini, Phys. Rev. C **80**, 064001 (2009).
[40] S. Bacca, N. Barnea, W. Leidemann, and G. Orlandini, Phys. Rev. Lett. **110**, 042503 (2013).
[41] N. Barnea, V. D. Efros, W. Leidemann, and G. Orlandini, Few Body Syst. **47**, 201 (2010).
[42] F. Ritz, H. Goller, T. Wilbois, and H. Arenhovel, Phys. Rev. C **55**, 2214 (1997).
[43] N. Rocco, A. Lovato, and O. Benhar, Phys. Rev. C **94**, 065501 (2016).
[44] W. M. Alberico, A. Molinari, T. W. Donnelly, E. L. Kronenberg, and J. W. Van Orden, Phys. Rev. C **38**, 1801 (1988).
[45] M. B. Barbaro, R. Cenni, A. De Pace, T. W. Donnelly, and A. Molinari, Nucl. Phys. A **643**, 137 (1998).
[46] O. Benhar, D. Day, and I. Sick, arXiv:nucl-ex/0603032, http://faculty.virginia.edu/qes-archive.